Nonautonomous Breather and Rogue Wave in Spinor Bose–Einstein Condensates with Space-Time Modulated Potentials

Cuicui Ding(丁崔崔)[1], Qin Zhou(周勤)[1,2*], Siliu Xu(徐四六)[3], Houria Triki[4], Mohammad Mirzazadeh[5], and Wenjun Liu(刘文军)[6*]

[1]*Research Group of Nonlinear Optical Science and Technology, School of Mathematical and Physical Sciences, Wuhan Textile University, Wuhan 430200, China*
[2]*State Key Laboratory of New Textile Materials and Advanced Processing Technologies, Wuhan Textile University, Wuhan 430200, China*
[3]*School of Biomedical Engineering and Medical Imaging, Xianning Medical College, Hubei University of Science and Technology, Xianning 437100, China*
[4]*Radiation Physics Laboratory, Department of Physics, Faculty of Sciences, Badji Mokhtar University, P. O. Box 12, 23000 Annaba, Algeria*
[5]*Department of Engineering Sciences, Faculty of Technology and Engineering, East of Guilan, University of Guilan, Rudsar-Vajargah, Iran*
[6]*State Key Laboratory of Information Photonics and Optical Communications, School of Science, Beijing University of Posts and Telecommunications, Beijing 100876, China*

(Received 8 February 2023; accepted manuscript online 3 March 2023)

To study controlled evolution of nonautonomous matter-wave breathers and rogue waves in spinor Bose–Einstein condensates with spatiotemporal modulation, we focus on a system of three coupled Gross–Pitaevskii equations with spacetime-dependent external potentials and temporally modulated gain-loss distributions. With different external potentials and gain-loss distributions, various solutions for controlled nonautonomous matter-wave breathers and rogue waves are derived by the Darboux transformation method, such as breathers and rogue waves on arched and constant backgrounds which have the periodic and parabolic trajectories. Effects of the gain-loss distribution and linear potential on the breathers and rogue waves are studied. Nonautonomous two-breathers on the arched and constant backgrounds are also derived.

DOI: 10.1088/0256-307X/40/4/040501

Spinor Bose–Einstein condensates (BECs) have attracted great interests of researchers since their experimental realization on the optically trapped ^{23}Na Bose condensate.[1–7] Spinor BECs with freedom of internal spin degrees possess abundant phenomena including magnetic crystallization, spin texture, and fractional vortices, which have no counterpart in magnetically trapped condensates with the spin degree being frozen.[7] Many experimental and theoretical studies on spinor BECs have revealed a variety of interesting phenomena, such as polar-to-ferromagnetic phase transitions, quantum knots, condensation of magnon excitations, and various kinds of nonlinear excitations consisting of dark/bright solitons, soliton complexes, rogue waves, and vortices, etc.[8,9] Applications of the matter-wave solitons in atom optics are expected to be atom laser, atom interferometry and coherent atom transport.[10,11] In addition, matter-wave solitons in atomic BECs may have more extensive applications because of their internal spin degrees of freedom,[12] which can produce multiple signals.

Recently, there has been an increasing interest for studying the time–space modulated BEC system with time–space dependent external harmonic potentials,[13,14] time-variant atom gain or loss distribution via optical pumping or depleting,[15] and time-dependent nonlinearity manipulated through the Feshbach resonance technique.[16,17] In the time–space modulated systems, nonautonomous breathers and rogue waves, which commonly propagate with varying amplitudes and velocities, can be obtained and can be extended to different physical systems including the hydrodynamics, nonlinear optics, and matter waves, etc.[17–22] Nonautonomous matter waves in the time–space modulated spinor BECs possess properties different from those of classical matter waves, which develops the concept of matter waves.[22,23]

In the present work, to study the nonautonomous matter waves of the spinor BEC with attractive mean field interaction and ferromagnetic spin-exchange interaction under the time–space modulated external potential and time-variant atom gain or loss distribution, we focus on the following scaled coupled Gross–Pitaevskii (GP) equations:[24]

$$i\frac{\partial\phi_{\pm1}}{\partial t} = -\frac{\partial^2\phi_{\pm1}}{\partial x^2} - 2(|\phi_{\pm1}|^2 + 2|\phi_0|^2)\phi_{\pm1} - 2\phi_0^2\phi_{\mp1}^* - U_{\rm trap}(x,t)\phi_{\pm1} - i\Gamma(t)\phi_{\pm1}, \tag{1a}$$

$$i\frac{\partial\phi_0}{\partial t} = -\frac{\partial^2\phi_0}{\partial x^2} - 2(|\phi_{+1}|^2 + |\phi_0|^2 + |\phi_{-1}|^2)\phi_0 - 2\phi_{-1}\phi_0^*\phi_{+1} - U_{\rm trap}(x,t)\phi_0 - i\Gamma(t)\phi_0, \tag{1b}$$

where the asterisk * represents the complex conjugation, ϕ_j $(j = -1, 0, +1)$ denote the three components of the spinor condensate wave function Φ with the scaled spatial

*Corresponding authors. Email: qinzhou@whu.edu.cn; jungliu@bupt.edu.cn
© 2023 Chinese Physical Society and IOP Publishing Ltd

and time coordinates x and t, and $U_{\rm trap}(x,t)=U_p(t)x^2+U_l(t)x$ is time–space modulated external potential,[22,25] $\Gamma(t)$ stands for the time-variant atom gain or loss distribution which corresponds to the mechanism of loading external atoms into the BEC by optical pumping or continuous depletion of atoms in the BEC.[26] Under special conditions, system (1) can reduce to the Manakov equations. A new class of breathers and rogue waves which are the non-degenerate breathers and rogue waves have been found in the vector systems.[27–29]

Lax pair and Darboux transformation (DT) for system (1) have been obtained to derive the nonautonomous matter wave solitons in our previous work.[30] Here, we adopt the previous Lax pair and DT to investigate the nonautonomous breathers and rogue waves. The nonisospectral Lax pair for system (1) has been derived as[30]

$$\begin{aligned}&\Psi_x=[i\lambda(t)J+P]\Psi,\\&\Psi_t=[2i\lambda(t)^2J+2\lambda(t)V_1+iV_0]\Psi,\end{aligned}\tag{2}$$

where $\lambda(t)$ is the complex nonisospectral parameter, $\Psi=(\mathcal{H},\mathcal{Y})^{\rm T}$ is the matrix eigenfunction corresponding to $\lambda(t)$, $\mathcal{H}$ and $\mathcal{Y}$ are 2×2 matrices, and other matrices are expressed as

$$\begin{aligned}&J=\begin{pmatrix}-I&O\\O&I\end{pmatrix},\quad P=\begin{pmatrix}O&Q\\-Q^\dagger&O\end{pmatrix},\\&V_0=\begin{pmatrix}QQ^\dagger&Q_x+2i\Gamma(t)xQ\\Q_x^\dagger-2i\Gamma(t)xQ^\dagger&-Q^\dagger Q\end{pmatrix},\\&V_1=-i\Lambda(x,t)J+P,\quad \Lambda(x,t)=\Big[\Gamma(t)+\frac{\gamma(t)}{4\lambda(t)}\Big]x,\\&Q=e^{-\frac{i\Gamma(t)x^2}{2}}\begin{pmatrix}\phi_{+1}&\phi_0\\\phi_0&\phi_{-1}\end{pmatrix},\\&\lambda(t)=\xi e^{-2\int\Gamma(t)dt}-\frac{1}{2}e^{-2\int\Gamma(t)dt}\int\gamma(t)e^{2\int\Gamma(t)dt}dt,\end{aligned}$$

I represents the 2×2 unit matrix, O denotes the 2×2 zero matrix, † means the Hermite conjugation, and ξ is a complex constant. We point out that the above Lax pair (2) is obtained under the integrable conditions $U_p(t)=\frac{1}{2}\Gamma_t(t)+\Gamma(t)^2$ and $U_l(t)=\gamma(t)$, where $\gamma(t)$ is an arbitrary real function of t. Let $\Psi_j=(\mathcal{H}_j^{[0]},\mathcal{Y}_j^{[0]})^{\rm T}$ ($j=1,2,3,\ldots$) be the complex matrix solutions of Lax pair (2) with $Q=Q[0]$ and $\lambda(t)=\lambda_j(t)$, we obtain the following Nth-step DT for system (1):[30]

$$\begin{aligned}\Psi[N]=&T[N]T[N-1]\cdots T[1]\Psi,\\T[j]=&\tau_j(\lambda)[\lambda I-H[j-1]\Lambda_jH[j-1]^{-1}],\end{aligned}\tag{3a}$$

$$\begin{aligned}Q[N]=&Q[0]-\sum_{j=1}^{N}2i(\lambda_j-\lambda_j^*)\big(\mathcal{Y}_j^{[j-1]}\mathcal{H}_j^{[j-1]^{-1}}\\&+\mathcal{H}_j^{[j-1]*}\mathcal{Y}_j^{[j-1]*^{-1}}\big)^{-1},\end{aligned}\tag{3b}$$

where

$$\begin{aligned}\Psi_j[j-1]=&(\mathcal{H}_j^{[j-1]},\mathcal{Y}_j^{[j-1]})^{\rm T}\\=&T[j-1]|_{\lambda=\lambda_j}T[j-2]|_{\lambda=\lambda_{j-1}}\cdots T[1]|_{\lambda=\lambda_2}\Psi_j,\\\tau_j(\lambda)=&[(\lambda(t)-\lambda_j(t))(\lambda(t)-\lambda_j^*(t))]^{-\frac{1}{2}},\\H[j-1]=&\begin{pmatrix}\mathcal{H}_j^{[j-1]}&-\mathcal{Y}_j^{[j-1]*}\\\mathcal{Y}_j^{[j-1]}&\mathcal{H}_j^{[j-1]*}\end{pmatrix},\quad \Lambda_j=\begin{pmatrix}\lambda_jI&O\\O&\lambda_j^*I\end{pmatrix}.\end{aligned}$$

In this Letter, we investigate the spinor BECs with time–space modulated external potentials and time-variant atom gain or loss distributions, and construct the analytical demonstration of the nonautonomous breathers and rogue waves using the Darboux transformation method. Under several different kinds of time–space modulated external potentials and time-varying gain or loss distributions, evolutions of the nonautonomous breathers and rogue waves will be analyzed analytically and graphically.

Nonautonomous Breathers. Next, utilizing the above Nth-step DT, we construct the nonautonomous breathers for system (1). To this end, we take the following nonzero seed solutions for system (1):

$$Q[0]=A_ce^{i[A(t)x+B(t)]-2\int\Gamma(t)dt},\tag{4}$$

which determine the nonzero background of the nonautonomous breathers, where

$$\begin{aligned}&A_c=\frac{1}{\sqrt{j_1^2+j_2^2}}\begin{pmatrix}j_1&j_2\\j_2&-j_1\end{pmatrix},\\&A(t)=e^{-2\int\Gamma(t)dt}\int\gamma(t)e^{2\int\Gamma(t)dt}dt,\\&B(t)=\int e^{-4\int\Gamma(t)dt}[2-(\int\gamma(t)e^{2\int\Gamma(t)dt}dt)^2]dt,\end{aligned}$$

j_1 and j_2 are both real constants. Then substituting seed solutions (4) into Lax pair (2), we derive the matrix eigenfunction $\Psi_1=(\mathcal{H}_1^{[0]},\mathcal{Y}_1^{[0]})^{\rm T}$ with $\lambda_1(t)=\xi_1e^{-2\int\Gamma(t)dt}-\frac{1}{2}e^{-2\int\Gamma(t)dt}\int\gamma(t)e^{2\int\Gamma(t)dt}dt$ as

$$\mathcal{H}_1^{[0]}=i\mathcal{K}(l_1e^{i\theta(x,t)}+l_2e^{-i\theta(x,t)})e^{\frac{i}{2}[A(t)x+B(t)]},\tag{5a}$$

$$\mathcal{Y}_1^{[0]}=A_c\mathcal{K}(l_3e^{i\theta(x,t)}+l_4e^{-i\theta(x,t)})e^{-\frac{i}{2}[A(t)x+B(t)]},\tag{5b}$$

where

$$\begin{aligned}\theta(x,t)=&\sqrt{1+\xi_1^2}e^{-2\int\Gamma(t)dt}x+2\sqrt{1+\xi_1^2}\\&\cdot\int e^{-4\int\Gamma(t)dt}\Big(\xi_1-\int\gamma(t)e^{2\int\Gamma(t)dt}dt\Big)dt,\\\mathcal{K}=&\begin{pmatrix}k_1&k_2\\k_2&k_3\end{pmatrix},\quad l_3=-l_1(\sqrt{1+\xi_1^2}+\xi_1),\\l_4=&l_2(\sqrt{1+\xi_1^2}-\xi_1),\end{aligned}$$

with l_1, l_2, ξ_1, k_1, k_2, and k_3 being all the complex constants.

Via substituting the seed solutions $Q[0]$ and matrix eigenfunction $\Psi_1=(\mathcal{H}_1^{[0]},\mathcal{Y}_1^{[0]})^{\rm T}$ into the Nth-step DT (3) with $N=1$, we can obtain the nonautonomous one-breather solutions for system (1). Additionally, under the parameter conditions $\mathcal{K}=\left(\begin{smallmatrix}1&0\\0&1\end{smallmatrix}\right)$ (i.e., $k_1=k_3=1,k_2=0$), $l_1=-l_2=1$ and $\xi_1=ih_1$ with h_1 being a real constant and $h_1\neq1$, a compact form of the nonautonomous one-breather solutions can be derived as

$$\begin{aligned}&Q[1]\\=&Q[0]\Big[1+\frac{4h_1\sin\theta(\sqrt{1-h_1^2}\cos\theta^*-h_1\sin\theta^*)}{\cosh(2\theta_{\rm I})-h_1^2\cos(2\theta_{\rm R})-h_1\sqrt{1-h_1^2}\sin(2\theta_{\rm R})}\Big].\end{aligned}\tag{6}$$

Here, $\theta_{\rm R}$ and $\theta_{\rm I}$ represent the real and imaginary parts of $\theta(x,t)$, respectively. It can be seen from the above solutions (6) that the three components ϕ_{+1}, ϕ_0, and ϕ_{-1} have the same respiratory structure and $|\phi_{\pm1}| = |\frac{j_1}{j_2}||\phi_0|$ under the above parameter conditions. However, when the matrix $\mathcal{K}$ takes the general form rather than identity matrix, the three components ϕ_{+1}, ϕ_0, and ϕ_{-1} will possess different structures, such as the kink breathers. Moreover, it can be seen that the gain/loss distributions $\Gamma(t)$ will significantly affect the background of the breather and the trajectory of the breather is determined by $\Gamma(t)$ and $\gamma(t)$ together from solutions (4) and solutions (6).

Nonautonomous Breathers without Effects of the Gain-Loss Distributions. In the following, we consider the influences of the gain/loss distributions $\Gamma(t)$ and linear potential $\gamma(t)$ on the breathers, respectively. From the seed solutions (4) and one-breather solutions (6), it can be found that $\Gamma(t)$ will directly affect the background of the breather while $\gamma(t)$ will not. In addition, we discover that kink breather can be obtained when none of the elements of the matrix $\mathcal{K}^* A_c \mathcal{K} A_c$ are zero. We next take $\Gamma(t) = 0$ while $\gamma(t) \neq 0$ to study the effect of $\gamma(t)$ on the breathers, as shown in Fig. 1. Here, we let the matrix $\mathcal{K}$ take the general form and special form (i.e., identity matrix) to get the kink and normal breathers separately. It can be seen that the breather has a kink shape background in Fig. 1(a), which is mostly called the kink breather while the breather with a constant background in Fig. 1(b) is called the normal breather. Moreover, according to the expression of $\theta(x,t)$, it has that the trajectory of the breather can be controlled by $\gamma(t)$ along the t axis. An intuitive example which reveals the breathers with cubic and periodic trajectories can be seen in Fig. 1 with $\gamma(t) = 0.01t$ and $\cos(0.8\,t)$, respectively. We point out that the nonconstant background of the kink breather in Fig. 1(a) is not caused by the gain-loss distributions but by the matrix $\mathcal{K}$. That is to say, there are two types of breathers in the system itself.

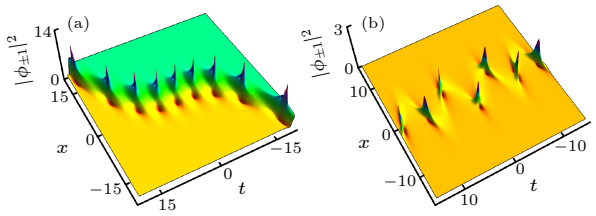

Fig. 1. Nonautonomous breathers with external potential $U_{\rm trap}(x,t) = \gamma(t)x$. (a) Kink breather with $k_1 = 1 + 0.5i$, $k_2 = -1 + 0.6i$, $k_3 = 0.5 - i$, and $\gamma(t) = 0.01t$. (b) Normal breather with $k_1 = k_3 = 1$, $k_2 = 0$, and $\gamma(t) = \cos(0.8\,t)$. Other parameters are $\Gamma(t) = 0$, $j_1 = \frac{1}{\sqrt{5}}$, $j_2 = \frac{2}{\sqrt{5}}$, and $\xi_1 = 1.05i$.

Nonautonomous Breathers with Effects of the Gain-Loss Distributions. We can take $\gamma(t) = 0$ while $\Gamma(t) \neq 0$ to investigate the effects of the gain-loss distributions on the nonautonomous breathers. Two kinds of nonautonomous breathers on the arched background, which are the Akhmediev breather (space-periodic breather) and Kuznetsov–Ma breather (time-periodic breather), have been obtained and shown in Fig. 2, where the gain-loss coefficient $\Gamma(t)$ is chosen as a linear function of t. In fact, according to the above one-breather solutions (6), one can find that the background of the breather will decrease or increase by exponentially modulating the gain-loss distribution $\Gamma(t) = \alpha_1$, where α_1 is a real nonzero constant. In addition, when $\Gamma(t) = \beta_1 t + \alpha_1$ with β_1 being a real constant, nonautonomous breathers on the arched background can be obtained, as shown in Fig. 2. It can be seen that the background decreases to the zero plane when $t \to \pm\infty$. More precisely, the arched background can be depicted by the function $\exp[-\beta_1(t + \frac{\alpha_1}{\beta_1})^2]$, from which one can see that β_1 can control the profile and steepness of the arched background and the ratio $\frac{\alpha_1}{\beta_1}$ can tune the hump of the arched background which has a translation relative to the line $t = 0$. In addition to the regulating on the background, there is an additional effect on the breather caused by the external potentials, as revealed in Fig. 2(b). The Kuznetsov–Ma breather along the direction of t axis will be cut off because of the arched background induced by the gain-loss distribution. In a word, the gain/loss distributions $\Gamma(t)$ will significantly affect the background of the breather, while the linear potential has no influence on the background of the breather, and the trajectory of the breather is determined jointly by $\Gamma(t)$ and $\gamma(t)$.

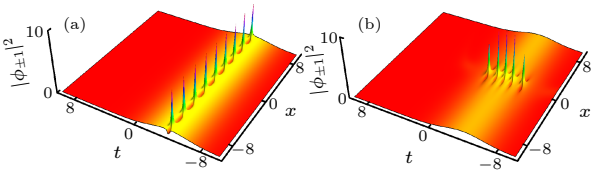

Fig. 2. Nonautonomous breathers on the arched background with external potential $U_{\rm trap}(x,t) = [\frac{1}{2}\Gamma_t(t) + \Gamma(t)^2]x^2$ and $\Gamma(t) = 0.05t + 0.2$. (a) Akhmediev breather with $\xi_1 = 0.8i$. (b) Kuznetsov–Ma breather with $\xi_1 = 1.05i$. Other parameters are $\gamma(t) = 0$, $j_1 = \frac{1}{\sqrt{5}}$, $j_2 = \frac{2}{\sqrt{5}}$, $k_1 = k_3 = 1$, and $k_2 = 0$.

To get the two nonautonomous breathers, one can derive, from the nonzero seed solution $Q[0]$ in Eq. (4), two matrix eigenfunctions, $\Psi_j = (\mathcal{H}_j^{[0]}, \mathcal{Y}_j^{[0]})^{\rm T}$ $(j = 1, 2)$ with $\lambda_j(t) = \xi_j e^{-2\int\Gamma(t)dt} - \frac{1}{2}e^{-2\int\Gamma(t)dt}\int\gamma(t)e^{2\int\Gamma(t)dt}dt$ as

$$\mathcal{H}_j^{[0]} = i\mathcal{K}_j(l_{1j}e^{i\theta_j(x,t)} + l_{2j}e^{-i\theta_j(x,t)})e^{\frac{i}{2}[A(t)x+B(t)]}, \quad (7a)$$

$$\mathcal{Y}_j^{[0]} = A_c\mathcal{K}_j(l_{3j}e^{i\theta_j(x,t)} + l_{4j}e^{-i\theta_j(x,t)})e^{-\frac{i}{2}[A(t)x+B(t)]}, \quad (7b)$$

where

$$\theta_j(x,t) = \sqrt{1+\xi_j^2}e^{-2\int\Gamma(t)dt}x + 2\sqrt{1+\xi_j^2} \cdot \int e^{-4\int\Gamma(t)dt}\Big(\xi_j - \int\gamma(t)e^{2\int\Gamma(t)dt}dt\Big)dt,$$

$$\mathcal{K}_j = \begin{pmatrix} k_{1j} & k_{2j} \\ k_{2j} & k_{3j} \end{pmatrix}, \quad l_{3j} = -l_{1j}(\sqrt{1+\xi_j^2} + \xi_j),$$

$$l_{4j} = l_{2j}(\sqrt{1+\xi_j^2} - \xi_j),$$

with l_{1j}, l_{2j}, ξ_j, k_{1j}, k_{2j}, and k_{3j} being all the complex constants. Utilizing the Nth-order DT (3) with $N = 2$, we can obtain the two-breather solutions for system (1). Considering that the respective expression is extremely ponderous, we do not display it here.

Nonautonomous two breathers are displayed in Fig. 3 with two different external potentials. To analyze the ef-

fects of linear potential coefficient $\gamma(t)$ and gain-loss coefficient $\Gamma(t)$ on the two breathers, we have taken $\mathcal{K}_1$ and $\mathcal{K}_2$ to be the identity matrices here for simplicity. In addition, spectral parameters ξ_1 and ξ_2 are chosen to be less than 1 and greater than 1, respectively, to obtain the interaction between one Akhmediev breather and one Kuznetsov–Ma breather. Similarly, when the gain-loss coefficient $\Gamma(t)$ is taken as the form $\Gamma(t)=\beta_1 t+\alpha_1$, the arched background for the two breathers can also be obtained as shown in Fig. 3(a). It can be seen that the Kuznetsov–Ma breather (time-periodic) is cut off because of the arched background induced by the gain-loss distribution, and the Akhmediev breather (space-periodic) is located at the hump of the arched background. When the linear potential coefficient $\gamma(t)$ is chosen as a constant and without the gain-loss distribution, the parabolic Kuznetsov–Ma breather together with a Akhmediev breather on the constant background can be obtained as displayed in Fig. 3(b). Since there is no gain-loss distribution, the background of the two-breathers will keep unchanged. Under the effect of $\gamma(t)$, the periodicity along the t axis of the Kuznetsov–Ma breather will be modulated. For both the cases in Fig. 3, a higher-order rogue wave with high amplitude has been excited by the interaction of two breathers.

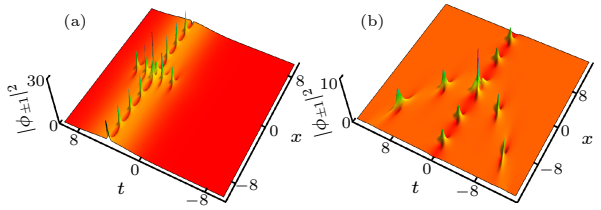

Fig. 3. (a) Nonautonomous two-breathers on the arched background with external potential $U_{\rm trap}(x,t)=[\frac{1}{2}\Gamma_t(t)+\Gamma(t)^2]x^2$ and $\Gamma(t)=0.05\,t-0.2$. (b) Nonautonomous Akhmediev and parabolic Kuznetsov–Ma breathers with external potential $U_{\rm trap}(x,t)=\gamma(t)x$, $\Gamma(t)=0$, and $\gamma(t)=-0.1$. Other parameters are $j_1=j_2=1$, $\mathcal{K}_1=\mathcal{K}_2=I_2$, $\xi_1=0.8i$, and $\xi_2=1.05i$.

Nonautonomous Rogue Waves. To get the nonautonomous rogue waves, one can obtain, from the nonzero seed solution $Q[0]$ in Eq. (4), the matrix eigenfunction $\Psi_1=(\mathcal{H}_1,\mathcal{Y}_1)^{\rm T}$ with ξ_1 being a pure complex constant and $\lambda_1(t)=ih_1e^{-2\int\Gamma(t)dt}-\frac{1}{2}e^{-2\int\Gamma(t)dt}\int\gamma(t)e^{2\int\Gamma(t)dt}dt$ as

$$\mathcal{H}_1=i\mathcal{K}(l_1e^{\theta(x,t)}-l_2e^{-\theta(x,t)})e^{\frac{i}{2}[A(t)x+B(t)]}, \tag{8a}$$

$$\mathcal{Y}_1=A_c\mathcal{K}(-l_2e^{\theta(x,t)}+l_1e^{-\theta(x,t)})e^{-\frac{i}{2}[A(t)x+B(t)]}, \tag{8b}$$

where

$$\theta(x,t)=\sqrt{h_1^2-1}e^{-2\int\Gamma(t)dt}x+2i\sqrt{h_1^2-1}\int e^{-4\int\Gamma(t)dt}\cdot\Big(h_1+i\int\gamma(t)e^{2\int\Gamma(t)dt}dt\Big)dt,$$

$$l_1=\frac{\sqrt{h_1+\sqrt{h_1^2-1}}}{\sqrt{h_1^2-1}},\quad l_2=\frac{\sqrt{h_1-\sqrt{h_1^2-1}}}{\sqrt{h_1^2-1}},$$

$$h_1=1+\epsilon_1^2,$$

and ϵ_1 is a real constant. Taking the expansion of matrix eigenfunction (8) at $\epsilon_1=0$, one can obtain

$$\mathcal{H}_1(\epsilon_1)=\mathcal{H}_1^{[0]}+\mathcal{H}_1^{[1]}\epsilon_1^2+\cdots, \tag{9a}$$

$$\mathcal{Y}_1(\epsilon_1)=\mathcal{Y}_1^{[0]}+\mathcal{Y}_1^{[1]}\epsilon_1^2+\cdots, \tag{9b}$$

where $\mathcal{H}_1^{[k]}=\frac{1}{(2k)!}\frac{\partial^{2k}}{\partial\epsilon_1^{2k}}\mathcal{H}_1(\epsilon_1)|_{\epsilon_1=0}$ and $\mathcal{Y}_1^{[k]}=\frac{1}{(2k)!}\frac{\partial^{2k}}{\partial\epsilon_1^{2k}}\mathcal{Y}_1(\epsilon_1)|_{\epsilon_1=0}$ $(k=0,1,2,\ldots)$. Accordingly, we can derive

$$\mathcal{H}_1^{[0]}=\mathcal{K}M_1e^{\frac{i}{2}[A(t)x+B(t)]-2\int\Gamma(t)dt}, \tag{10a}$$

$$\mathcal{Y}_1^{[0]}=A_c\mathcal{K}M_2e^{-\frac{i}{2}[A(t)x+B(t)]-2\int\Gamma(t)dt}, \tag{10b}$$

where

$$M_1=2x+e^{2\int\Gamma(t)dt}\cdot\Big[1+4i\int e^{-4\int\Gamma(t)dt}\Big(1+i\int\gamma(t)e^{2\int\Gamma(t)dt}dt\Big)dt\Big],$$

$$M_2=-2x+e^{2\int\Gamma(t)dt}\cdot\Big[1-4i\int e^{-4\int\Gamma(t)dt}\Big(1+i\int\gamma(t)e^{2\int\Gamma(t)dt}dt\Big)dt\Big].$$

Matrix eigenfunction $\Psi_1^{[0]}=(\mathcal{H}_1^{[0]},\mathcal{Y}_1^{[0]})^{\rm T}$ given in Eq. (10) can be directly verified as a solution of Lax pair (2) with the seed solution (4) and spectral parameter $\lambda_1(t)=ie^{-2\int\Gamma(t)dt}-\frac{1}{2}e^{-2\int\Gamma(t)dt}\int\gamma(t)e^{2\int\Gamma(t)dt}dt$. Then, substituting the seed solutions $Q[0]$ in Eq. (4) and matrix eigenfunction $\Psi_1^{[0]}=(\mathcal{H}_1^{[0]},\mathcal{Y}_1^{[0]})^{\rm T}$ in Eq. (10) into the Nth-step DT (3) with $N=1$, we can obtain the nonautonomous rogue-wave solutions for system (1). Additionally, under the parameter condition $\mathcal{K}=\left(\begin{smallmatrix}1&0\\0&1\end{smallmatrix}\right)$ (i.e., $k_1=k_3=1, k_2=0$), a compact form of the nonautonomous rogue-wave solutions can be derived as

$$Q[1]=A_c\Big(1+\frac{4M_1M_2^*}{|M_1|^2+|M_2|^2}\Big)e^{i[A(t)x+B(t)]-2\int\Gamma(t)dt}. \tag{11}$$

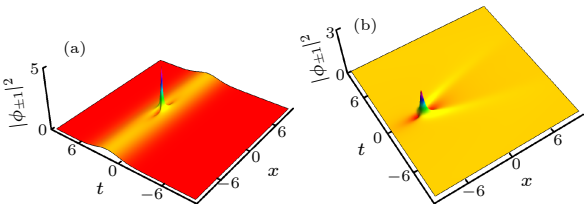

Fig. 4. (a) Nonautonomous rogue wave on the arched background with external potential $U_{\rm trap}(x,t)=[\frac{1}{2}\Gamma_t(t)+\Gamma(t)^2]x^2$ and $\Gamma(t)=0.1\,t-0.2$. (b) Nonautonomous rogue wave with external potential $U_{\rm trap}(x,t)=\gamma(t)x$, $\Gamma(t)=0$, and $\gamma(t)=\cos(0.6\,t)$. Other parameters are $j_1=\frac{1}{\sqrt{5}}$ and $j_2=\frac{2}{\sqrt{5}}$.

From solutions (11), it can be found that the three components ϕ_{+1}, ϕ_0 and ϕ_{-1} have the same structure and $|\phi_{\pm1}|=|\frac{j_1}{j_2}||\phi_0|$ under the above parameter conditions, so that we have only displayed the components ϕ_{+1} and ϕ_{-1} together as an example in Fig. 4. We separately consider the cases $\Gamma(t)\neq0$ and $\gamma(t)\neq0$ to investigate the influence of the gain-loss distribution and linear potential on the nonautonomous rogue waves. Firstly, we set $\Gamma(t)=\beta_1t+\alpha_1$ and $\gamma(t)=0$, and obtain the rogue wave on the arched background, as shown in Fig. 4(a). Different

from the autonomous rogue waves without the gain-loss distribution, the nonautonomous rogue wave in Fig. 4(a) is not located at the origin but has a shift and located at $(x = 0, t = -\frac{\alpha_1}{\beta_1})$. In addition, under the effect of gain-loss distribution, the amplitude of the rogue wave will be different. Next, we set $\gamma(t) = \rho_1 \cos(\rho_2 t)$ and $\Gamma(t) = 0$ to study the modulation of the linear potential coefficient $\gamma(t)$ on the nonautonomous rogue wave, as shown in Fig. 4(b). It can be seen that the background keep unchanged but the rogue wave becomes deformed and has a shift on the background under the modulation of the linear potential coefficient $\gamma(t)$.

In summary, spinor BECs with time–space modulated external potentials and time-variant atom gain or loss distribution have been investigated, and the analytical demonstration of the nonautonomous breathers and rogue waves has been constructed by the Darboux transformation method. Under several different kinds of time–space modulated external potentials and time-varying gain-loss distributions, evolutions of different nonautonomous breathers and rogue waves have been analyzed analytically and graphically. For example, nonautonomous breathers with the kink shape and constant background have been obtained with different parameters. Considering the gain-loss distribution and linear potential separately, we analyze the effects of $\Gamma(t)$ and $\gamma(t)$ on the nonautonomous breathers and find that $\Gamma(t)$ can influence the background of the breather while $\gamma(t)$ will affect the trajectory of the breather. Nonautonomous two-breathers on the arched background and constant background have also been obtained. By taking the limit of the breathers, nonautonomous rogue waves are derived.

Acknowledgements. This work was supported by the National Natural Science Foundation of China (Grant Nos. 11975172 and 12261131495).

References

[1] He J T, Fang P P, and Lin J 2022 *Chin. Phys. Lett.* **39** 020301
[2] Zhang Y L, Jia C Y, and Liang Z X 2022 *Chin. Phys. Lett.* **39** 020501
[3] Zhao Y, Lei Y B, Xu Y X, Xu S L, Triki H, Biswas A, and Zhou Q 2022 *Chin. Phys. Lett.* **39** 034202
[4] Zhou Q, Zhong Y, Triki H, Sun Y Z, Xu S L, Liu W J, and Biswas A 2022 *Chin. Phys. Lett.* **39** 044202
[5] Guo H, Qiu X, Ma Y, Jiang H F, and Zhang X F 2021 *Chin. Phys. B* **30** 060310
[6] Chen S L, Wang L X, Wen L, Dai C Q, Liu J K, and Zhang X F 2021 *Optik* **247** 167932
[7] Evrard B, Qu A, Dalibard J, and Gerbier F 2021 *Science* **373** 1340
[8] Borgh M O, Lovegrove J, and Ruostekoski J 2017 *Phys. Rev. A* **95** 053601
[9] Ollikainen T, Masuda S, Mottonen M, and Nakahara M 2017 *Phys. Rev. A* **95** 013615
[10] Meystre P 2001 *Atom Optics* (New York: Springer-Verlag)
[11] Sekh G A, Pepe F V, Facchi P, Pascazio S, and Salerno M 2015 *Phys. Rev. A* **92** 013639
[12] Chai X, Lao D, Fujimoto K, Hamazaki R, Ueda M, and Raman C 2020 *Phys. Rev. Lett.* **125** 030402
[13] Zhang X F, Hu X H, Liu X X, and Liu W M 2009 *Phys. Rev. A* **79** 033630
[14] Rajendran S, Muruganandamb P, and Lakshmanana M 2010 *Physica D* **239** 366
[15] Atre R, Panigrahi P K, and Agarwal G S 2006 *Phys. Rev. E* **73** 056611
[16] Yan M, DeSalvo B J, Ramachandhran B, Pu H, and Killian T C 2013 *Phys. Rev. Lett.* **110** 123201
[17] Shen Y J, Gao Y T, Zuo D W, Sun Y H, Feng Y J, and Xue L 2014 *Phys. Rev. E* **89** 062915
[18] Zhong Y, Triki H, and Zhou Q 2023 *Commun. Theor. Phys.* **75** 025003
[19] Qi Z Q, Zhang Z, and Li B 2021 *Chin. Phys. Lett.* **38** 060501
[20] Li J C, Chen J C, and Li B 2022 *Nonlinear Dyn.* **107** 781
[21] Jiang L, Li X, and Li B 2022 *Phys. Scr.* **97** 115201
[22] Serkin V N, Hasegawa A, and Belyaeva T L 2007 *Phys. Rev. Lett.* **98** 074102
[23] Yang Z Y, Zhao L C, Zhang T, Feng X Q, and Yue R H 2011 *Phys. Rev. E* **83** 066602
[24] Ieda J, Miyakawa T, and Wadati M 2004 *Phys. Rev. Lett.* **93** 194102
[25] Serkin V N, Hasegawa A, and Belyaeva T L 2010 *Phys. Rev. A* **81** 023610
[26] Janis J, Banks M, and Bigelow N P 2005 *Phys. Rev. A* **71** 013422
[27] Che W J, Chen S C, Liu C, Zhao L C, and Akhmediev N 2022 *Phys. Rev. A* **105** 043526
[28] Liu C, Chen S C, Yao X K, and Akhmediev N 2022 *Physica D* **433** 133192
[29] Liu C, Chen S C, Yao X K, and Akhmediev N 2022 *Chin. Phys. Lett.* **39** 094201
[30] Ding C C, Zhou Q, Xu S L, Sun Y Z, Liu W J, Mihalache D, and Malomed B A 2023 *Chaos Solitons Fractals.* **169** 113247